Kinetics of the Reaction of NO_3 with HO_2

Ian W. Hall, Richard P. Wayne,

Physical Chemistry Laboratory, University of Oxford, Oxford, U.K.

Richard A. Cox,* Michael E. Jenkin, and Garry D. Hayman

Harwell Laboratory, Didcot, Oxfordshire, U.K. *(Received: November 23, 1987)*

The kinetics of the title reaction were investigated by molecular modulation–UV/visible absorption spectroscopy. NO_3 and HO_2 were generated by modulated photolysis of Cl_2 in the presence of $ClONO_2$, H_2, and O_2 in a flow system at 1 atm pressure and their concentration modulations monitored by time-resolved absorption at 662 and 220 nm, respectively. The rate coefficient for the overall reaction $NO_3 + HO_2 \rightarrow$ products, k_4, was determined by computer fitting to data at five temperatures in the range 263–338 K and was given by $k_4 = (2.3^{+2.8}_{-1.8}) \times 10^{-12} \exp(+(170 \pm 270)/T)$ cm^3 molecule^{-1} s^{-1}. An upper limit of 0.6 for the ratio k_{4b}/k at 283 K, where k_{4b} is the rate constant for the reaction channel $NO_3 + HO_2 \rightarrow OH + NO_2 + O_2$, was established by measurement of OH by modulated resonance absorption. The alternate channel, 4a, is assumed to produce HNO_3, i.e., $NO_3 + HO_2 \rightarrow HNO_3 + O_2$.

Introduction

Assessment of the role played by NO_3 radicals in atmospheric chemistry requires accurate kinetic and photochemical data for reactions of NO_3 radicals with other atmospheric trace molecules. Recently a large number of new studies of NO_3 photochemistry and kinetics have been reported. Rate constants for NO_3 reactions with a range of organic molecules have been determined at room temperature by relative rate techniques.[1,2] Several of these reactions have now been investigated by direct methods and the rate constant values confirmed.[3–5] Rate constants for reactions of NO_3 with several gaseous inorganic molecules, e.g., CO, SO_2, H_2S, H_2O_2, NO, NO_2, and ClO, have also been determined with direct methods.[6–11] A pattern of reactivity for NO_3 is emerging from these studies which show that NO_3 reaction with closed-shell molecules is generally slower than similar reactions of OH, Cl, O, etc. but that NO_3 reacts rapidly with other radicals.

We have investigated the kinetics of NO_3 reactions using the reaction of Cl atoms, produced by photolysis of Cl_2 in the near-UV region, with chlorine nitrate as a source of NO_3 radicals:[11,12]

$$Cl + ClONO_2 \rightarrow Cl_2 + NO_3 \quad (1)$$

Rate coefficients for the reactions

$$Cl + NO_3 \rightarrow ClO + NO_2 \quad (2)$$

$$ClO + NO_3 \rightarrow ClOO + NO_2 \quad (3)$$

were determined from observations of the kinetic behavior of NO_3 and ClO in the modulated photolysis of Cl_2–$ClONO_2$–N_2 mixtures at 1 atm total pressure in a flow system.[11]

Information on the reactivity of NO_3 toward other radicals has been extended in the present work, by determination of the kinetics of the reaction of NO_3 with HO_2, which may occur by two exothermic channels:

$$NO_3 + HO_2 \rightarrow HNO_3 + O_2 \qquad \Delta H° = -218.9 \text{ kJ mol}^{-1} \quad (4a)$$

$$\rightarrow OH + NO_2 + O_2 \qquad \Delta H° = -11.6 \text{ kJ mol}^{-1} \quad (4b)$$

Reaction 4a could provide a significant route for conversion of active NO_x molecules to HNO_3 in the stratosphere, whereas reaction 4b could provide a route for conversion of HO_2 to the more reactive odd hydrogen radical, OH. Evidence for the reaction of NO_3 with HO_2 has been observed in the photolysis of HNO_3,[13] and this reaction has also been proposed as a sink for NO_3 in the NO_3 + HCHO reaction system.[14]

The kinetics of reaction 4 were investigated by the molecular modulation technique, using photochemically generated Cl atoms to produce NO_3 via reaction 1 and HO_2 via reaction of Cl with H_2:

$$Cl + H_2 \rightarrow HCl + H \quad (5)$$

$$H + O_2 + M \rightarrow HO_2 + M \quad (6)$$

NO_3 was monitored by absorption at 662 nm and HO_2 at 220 nm. The rate coefficient k_4 was determined from measurements of the kinetics of NO_3 decay in the presence of HO_2, and also by computer simulation of the modulated absorption wave forms for NO_3 and HO_2, using a detailed chemical description of the photolysis system.

Experimental Section

The molecular modulation spectrometer was used in the same configuration as described in detail before.[15] The experiments were performed in a quartz reaction cell, 120 cm long and 30 mm in diameter, illuminated by up to six "blacklights", ($\lambda = 350 \pm 50$ nm), driven by a square-wave modulated power supply.

The light intensity was monitored on a photodiode, mounted in a fixed position on the cell housing. The cell was jacketed and

(1) Atkinson, R.; Plum, C. N.; Carter, W. P. L.; Winer, A. M.; Pitts, J. N., Jr. *J. Phys. Chem.* **1984**, *88*, 1210.
(2) Atkinson, R.; Aschmann, S. M.; Goodman, M. A. *Int. J. Chem. Kinet.* **1987**, *19*, 299.
(3) Wallington, T. J.; Atkinson, R.; Winer, A. M.; Pitts, J. N., Jr. *J. Phys. Chem.* **1986**, *90*, 4640; **1986**, *90*, 5393.
(4) Ravishankara, A. R.; Mauldin, R. L., III *J. Phys. Chem.* **1985**, *89*, 3144.
(5) Tyndall, G. S.; Burrows, J. P.; Schneider, W.; Moortgat, G. K. *Chem. Phys. Lett.* **1986**, *130*, 463.
(6) Burrows, J. P.; Tyndall, G. S.; Moortgat, G. K. *J. Phys. Chem.* **1985**, *89*, 4848.
(7) Sander, S. P.; Kircher, C. C. *Chem. Phys. Lett.* **1986**, *126*, 149.
(8) Hammer, P. D.; Dlugokencky, E. J.; Howard, C. J. *J. Phys. Chem.* **1986**, *90*, 2491.
(9) Kircher, C. C.; Margitan, J. J.; Sander, S. P. *J. Phys. Chem.* **1984**, *88*, 4370.
(10) Smith, C. A.; Ravishankara, A. R.; Wine, P. H. *J. Phys. Chem.* **1985**, *89*, 1423.
(11) Cox, R. A.; Fowles, M.; Moulton, D.; Wayne, R. P. *J. Phys. Chem.* **1987**, *91*, 3361.
(12) Cox, R. A.; Barton, R. A.; Ljungstrom, E.; Stocker, D. W. *Chem. Phys. Lett.* **1984**, *108*, 228.
(13) Burrows, J. P.; Tyndall, G. S.; Schneider, W.; Moortgat, G. K.; Poulet, G.; Lebras, G. Presented at the XVII Informal Conference on Photochemistry, Boulder, CO, 1986.
(14) Cantrell, C. A.; Stockwell, W. R.; Anderson, L. G.; Busarow, K. L.; Perner, D.; Schmeltekopf, A.; Calvert, J. G.; Johnston, H. S. *J. Phys. Chem.* **1985**, *89*, 139.
(15) Jenkin, M. E.; Cox, R. A. *J. Phys. Chem.* **1985**, *89*, 192.

0022-3654/88/2092-5049$01.50/0

the temperature controlled to within ±0.5 °C by circulation of a thermostatically regulated glycol–water mixture through the jacket. Absorption was measured on a light beam passing through the long axis of the cell, which was dispersed by use of a 0.5-m monochromator (B&M Spectronik) and detected on a photomultiplier with enhanced sensitivity to red light (EMI 9781 R). The light sources were either a D_2 lamp for UV measurements or a tungsten filament lamp for measurement of NO_3 in the visible region. The signal was stored on a fast digital multichannel scaler (for modulated absorption) and also displayed on a chart recorder. The multichannel scaler was timed synchronously with the operation of the photolysis lamps and allowed accumulation of the modulated wave form during successive photolysis cycles.

The kinetics experiments were carried out with gas mixtures containing Cl_2 + $ClONO_2$ + H_2 + O_2 diluted in N_2 flowing through the reaction cell from a manifold at 1 atm pressure. The volumetric flow rate was 43.3 cm^3 s^{-1} at STP giving a residence time of approximately 25 s in the cell. Absorption measurements were made in the flowing system under modulated photolysis for averaging times up to 3000 s. All gas flows were controlled with an electronic mass flow controller (MKS Model 280), except for the Cl_2 which was metered through a precision needle valve and a calibrated rotameter.

Chlorine nitrate was prepared from the reaction of Cl_2O and N_2O_5 and purified by distillation and collection at −120 °C (bromoethane/liquid N_2). The purified liquid $ClONO_2$ was transferred to a bubbler held at −78 °C and the vapor carried into the flow manifold in a stream of N_2. The vapor pressure of $ClONO_2$ at −78 °C was sufficient to provide the required concentrations in the gas mixture (typically (0.6–10.0) × 10^{14} molecules cm^{-3}). All other gases were taken directly from cylinders: Cl_2 was used as a 5% mixture in high-purity N_2, and the Cl_2 concentration in the reaction cell was typically 1.5 × 10^{16} molecules cm^{-3}. O_2 concentrations were in the range (2.0–5.0) × 10^{17} molecules cm^{-3} and H_2 up to 6 × 10^{17} molecules cm^{-3}.

Chlorine nitrate and Cl_2 concentrations in the cell were measured before and during each kinetic experiment from their absorption at 220 and 350 nm, respectively. HO_2 was monitored in the modulation experiments at 220 nm, where its absorption was superimposed on that of $ClONO_2$ which had to be subtracted to obtain the modulated absorption wave form for HO_2. NO_3 measurements were made at 662 nm with a spectral resolution of 0.47 nm. All experiments were carried out at atmospheric pressure, and five temperatures in the range 263–348 K were used to investigate the temperature dependence of k_4.

Results

Preliminary experiments were carried out to investigate the kinetic behavior of NO_3 in mixtures containing different ratios of [$ClONO_2$] to [H_2]. In the absence of H_2, the chemical loss processes for NO_3 are very slow and NO_3 absorption exhibited large, low-frequency modulation resulting from intermittent photochemical production and flow-out from the cell. As [H_2] was increased, the NO_3 absorption decreased and at the same time the NO_3 lifetime decreased, so that a steady-state concentration of NO_3 was reached with a modulation period of <2 s; a typical wave form at high [H_2]/[$ClONO_2$] is shown in Figure 1. It is clear from these observations that there are additional reactions leading to loss of NO_3 when H_2 is present.

Possible reactions of NO_3 with H-containing species in addition to reaction 4 are

$$NO_3 + H \rightarrow OH + NO_2 \quad (7)$$

$$NO_3 + OH \rightarrow HO_2 + NO_2 \quad (8)$$

$$NO_3 + H_2 \rightarrow HNO_3 + H \quad (9)$$

$$NO_3 + H_2O_2 \rightarrow HNO_3 + HO_2 \quad (10)$$

The hydrogen peroxide is produced in the reaction

$$HO_2 + HO_2 \rightarrow H_2O_2 + O_2 \quad (11)$$

which dominates HO_2 kinetics in the Cl_2–H_2–O_2 system and

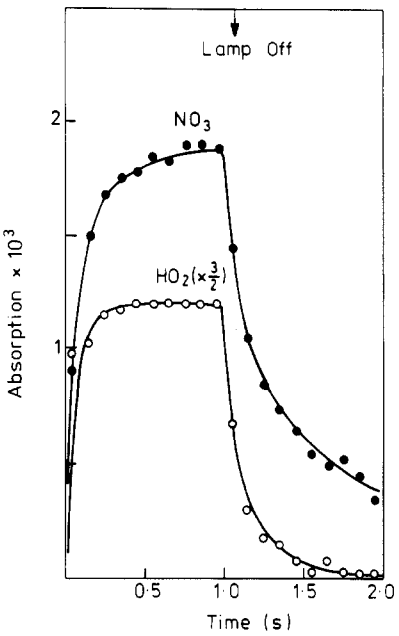

Figure 1. Modulated absorption–time profiles for NO_3 (at 662 nm) and HO_2 (at 220 nm) in the photolysis of Cl_2 (9.4 × 10^{15} molecules cm^{-3})–H_2 (5.0 × 10^{17} molecules cm^{-3})–$ClONO_2$ (0.98 × 10^{14} molecules cm^{-3})–O_2 (4 × 10^{17} molecules cm^{-3}) in 1 atm of N_2. Temperature = 308 K. Curves show computer simulations with k_{4a} = 0.6 × 10^{-12} cm^3 $molecule^{-1}$ s^{-1} and k_{4b} = 3.1 × 10^{-12} cm^3 $molecule^{-1}$ s^{-1}.

competes against reaction 4 for HO_2 in the present system. Distinction between reactions 4, 9, and 10 can be made from the kinetics of NO_3 decay. Since H_2 was in great excess over all other reagents, its average concentration in the reaction cell remained constant, to a first approximation, during the light-on and light-off periods of modulated photolysis. Thus NO_3 would follow pseudo-first-order kinetics if its removal were dominated by reaction 9. Similar behavior would be expected if reaction with H_2O_2 were important, but only when HO_2 (and hence H_2O_2) was produced in excess over NO_3, i.e., at relatively high [H_2]/[$ClONO_2$] ratios, so that the average [H_2O_2] was approximately constant during the modulation cycle. However, recent measurements[6] show that reaction 10 is relatively slow (k_{10} < 2.0 × 10^{-15} cm^3 $molecule^{-1}$ s^{-1} at 298 K) and is therefore unlikely to be a significant loss reaction for NO_3 in our system.

Figure 2 shows a semilog plot of the decay in NO_3 absorption vs time during the dark part of the modulation cycle, at four different initial HO_2 steady-state concentrations. The residual absorption corresponding to the NO_3 present at the end of the cycle was added to the NO_3 absorption at each time point and the NO_3 absorption at time t was normalized to the "initial" NO_3 absorption, i.e., at the end of the "light-on" part of the photolysis cycle. The residual absorption was estimated from the chart record of absorption at 662 nm and was typically about 1 × 10^{-3} absorption units, i.e., 20%–50% of the total absorption under these conditions. It will be seen from Figure 2 that the semilog plots are strongly curved, the pseudo-first-order rate constant k^I (=−d ln [NO_3]/dt) falling off rapidly with time even at the highest [HO_2]. This behavior strongly suggests that NO_3 is reacting with another radical in the system, which is itself decaying rapidly; reaction of NO_3 with H, OH or HO_2 might be expected to give this behavior.

Although the reaction of H atoms with NO_3 is extremely rapid (preliminary results from our laboratory give k_7 = 1.2 × 10^{-10} cm^3 $molecule^{-1}$ s^{-1} at 298 K), this reaction cannot provide a significant loss process for NO_3 since [H] is maintained at a very low level (≈10^8 molecules cm^{-3}) due to the fast reactions of H with O_2 and Cl_2.

Similarly the reaction of OH with NO_3 for which Mellouki et al.[16] report a rate coefficient of k_8 = (2.6 ± 0.5) × 10^{-11} cm^3

(16) Mellouki, A.; Le Bras, G.; Poulet, G. *J. Phys. Chem.* **1988**, *92*, 2229.

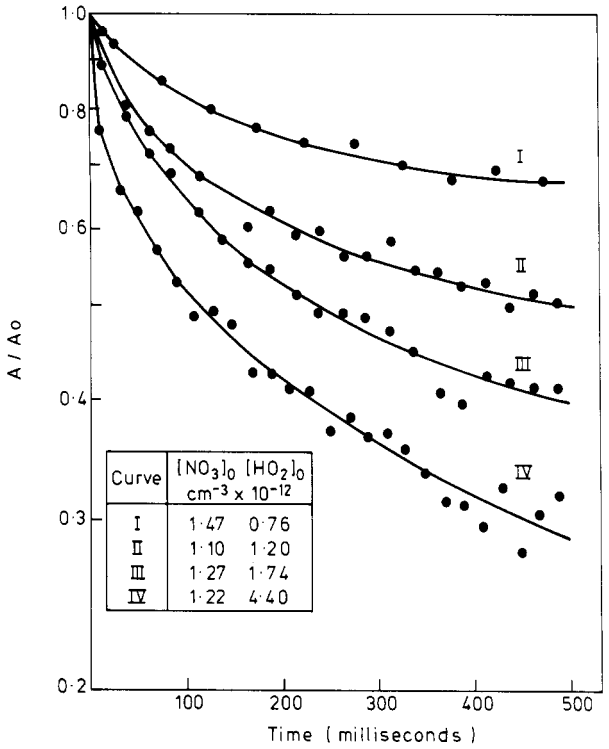

Figure 2. Semilog plot of decay in NO_3 absorption vs time. NO_3 absorption normalized to initial NO_3 concentration at end of "light on" period, which is given in box together with initial HO_2 concentration in units of molecules cm^{-3}.

molecule^{-1} s^{-1} can only be of minor importance due to the low steady-state [OH] present in the system (q.v.). The most likely NO_3 loss reaction is therefore reaction 4.

Figure 1 also shows the modulated absorption due to HO_2 at 220 nm, after correction for the component due to $ClONO_2$. HO_2 rapidly attains a steady state during the "light-on" period and decays to a low value in the dark, due to removal by reaction 4 with NO_3 and the self-reaction, reaction 11. The reaction of NO_3 with HO_2 would therefore explain the kinetic behavior of both of these radicals.

There are two exothermic channels for reaction 4. If HNO_3 is formed, in reaction 4a, one NO_3 and one HO_2 radical are removed. The alternate pathway forming NO_2 and OH leads to a more complex situation; NO_2 can subsequently react with NO_3 or HO_2 in the reversible reactions

$$NO_2 + NO_3 + M = N_2O_5 + M \quad (12)$$

$$NO_2 + HO_2 + M = HO_2NO_2 + M \quad (13)$$

leading to loss of a second NO_3 or an HO_2 radical. However, OH will react mainly with H_2, leading to regeneration of HO_2:

$$OH + H_2 \rightarrow H_2O + H \quad (14)$$

$$H + O_2 + M \rightarrow HO_2 + M \quad (6)$$

Alternatively, OH reacts with Cl_2, producing HOCl and Cl, the latter subsequently regenerating either NO_3 or HO_2. If HNO_3

$$OH + Cl_2 \rightarrow HOCl + Cl \quad (15)$$

is formed in reaction 4, the radicals are removed by reactions between HO_2 and NO_3, whereas if OH is formed, the overall loss rate of NO_3 (and HO_2) may be less and will not reflect the true rate of reaction 4.

Experiments were conducted to detect OH radicals produced in reaction 4 by searching for modulated absorption of resonance radiation from a conventional microwave-powered discharge lamp containing moist Ar. The setup was optimized by using the 254-nm photolysis of O_3–H_2O–He mixtures to produce OH ($\sim 10^{11}$ molecules cm^{-3}) in the cell. At 1 atm pressure and a spectral slit width of 0.13 nm, the effective cross section for absorption of resonance radiation was close to 1×10^{-16} cm^2 molecule^{-1},[18] giving a detection limit of approximately 5×10^9 OH molecules cm^{-3}. This corresponds to an absorbance of 6×10^{-5}, which was the minimum that could be clearly distinguished from the noise.

Several experiments were performed at 283 K to detect OH, utilizing H_2 concentrations lower than those used for the kinetics experiments, to reduce the loss rate of OH through the reaction

$$OH + H_2 \rightarrow H_2O + H \quad (16)$$

No modulated OH absorption could be detected in any of the experiments, indicating that the steady-state concentration of OH during photolysis was less than 5×10^9 molecules cm^{-3}. Computer simulations using the mechanism discussed below showed that for the lowest $[H_2]$ (5.2×10^{16} molecules cm^{-3}), the concentration modulation of OH would have exceeded the detection limit if $k_{4b}/k_4 > 0.6$. If reaction 4b was the exclusive pathway for the $HO_2 + NO_3$ reaction, the steady-state concentration of OH was predicted to be 7.5×10^9 molecules cm^{-3}. Because the calculated OH is close to the detection limit, a firm conclusion regarding the products of reaction 4 cannot be made but the results indicate that OH formation is not the exclusive pathway.

An estimate for the overall rate constant k_4 can be obtained from the kinetic data for NO_3 and HO_2 such as those shown in Figure 1. In this case, the steady-state absorptions of HO_2 and NO_3 at the end of the "light-on" period correspond to concentrations of 1.5×10^{12} and 0.82×10^{12} molecules cm^{-3}, respectively. Thus, in this experiment, the initial HO_2 concentration was approximately double that of NO_3, although the decay rate for HO_2 was more rapid, so that by the end of the cycle $[NO_3]$ was greater than $[HO_2]$. If NO_3 is removed only by reaction 4 and HO_2 by reactions 4 and 11, the initial decay of the radicals on cessation of photolysis is given by

$$-[d \ln [NO_3]/dt]_0 = k_4[HO_2]_{ss} \quad (i)$$

$$-[d \ln [HO_2]/dt]_0 = k_4[NO_3]_{ss} + 2k_{11}[HO_2]_{ss} \quad (ii)$$

Equations i and ii are based on the assumption that the products of reaction 4 do not regenerate or consume NO_3 or HO_2 on a fast time scale; as noted above, this assumption would not be entirely valid if OH formation was a major channel of reaction 4, since HO_2 and NO_3 would be regenerated. The initial logarithmic decay rates for NO_3 and HO_2 were 5.7 s^{-1} and 11.2 s^{-1}, which together with the observed steady-state values and the appropriate value for k_{11} ($=2.55 \times 10^{-12}$ cm^3 molecule^{-1} s^{-1} at 308 K and 1 atm pressure) give:

from eq i: $k_4 = 3.8 \times 10^{-12}$ cm^3 molecule^{-1} s^{-1}

from eq ii: $k_4 = 4.4 \times 10^{-12}$ cm^3 molecule^{-1} s^{-1}

Analysis of all of the HO_2 and NO_3 wave forms at five temperatures in the range of 263–348 K was conducted according to eq i and ii, and the results are summarized in Table I. The values of k_4 were reasonably reproducible, and although analysis by eq ii was intrinsically less accurate than that by i in view of the component due to the self-reaction of HO_2, there was good agreement between the two sets. The average values show no marked temperature dependence.

In view of the complex chemistry in the Cl_2–$ClONO_2$–H_2–O_2 photolysis system and the probability of reactions other than reaction 4 and 5 influencing the formation and decay of NO_3 and HO_2, computer simulation techniques were used to obtain values of k_4 which gave the best fit to the measured HO_2 and NO_3 absorption profiles. The simulations were performed by using the Harwell program FACSIMILE to integrate the differential equations governing molecular concentrations and find the values of specified

(17) Burrows, J. P.; Cox, R. A.; Derwent, R. G. *J. Photochem.* **1981**, *16*, 147.

(18) NASA Panel for Data Evaluation. *Chemical Kinetics and Photochemical Data for Use in Stratospheric Modelling*; JPL Publication 85-37; Jet Propulsion Laboratory: Pasadena, CA, 1985.

TABLE I: Experimental Data for $NO_3 + HO_2$ Reaction in the Modulated Photolysis of Cl_2–H_2–$ClONO_2$–O_2–N_2 Mixtures[a]

$[HO_2]_{ss}/10^{12}$ molecules/cm^{-3}[b]	$[NO_3]_{ss}/10^{12}$ molecules cm^{-3}[b]	$k^1_{NO_3}/s^{-1}$[c]	$k^1_{HO_2}/s^{-1}$[c]	$k_4/10^{-12}$ cm^3 molecule^{-1} s^{-1} k_{NO_3}[d]	k_{HO_2}[d]	k_{fit}[e]
		263 K				
0.77	0.99	3.1	11.0	4.1	4.6	6.0 ± 0.7
0.85	1.41	4.4	16.1	4.8	6.4	6.9 ± 0.3
						6.5 ± 0.5[f]
		283 K				
1.06	1.54	4.4	15.4	4.2	5.4	5.5 ± 1.0
1.27	1.10	5.0	17.8	3.9	8.4	4.9 ± 0.6
1.38	1.80	4.2	15.4	3.0	4.4	3.9 ± 0.3
1.74	1.27	7.7	12.6	4.4	0.7	4.0 ± 0.4
0.76	1.47	2.6	12.6	3.4	5.1	5.3 ± 1.2
1.06	1.69	5.2	13.8	5.1	4.3	4.6 ± 2.0
						4.7 ± 0.8[f]
		308 K				
1.50	0.82	5.7	11.2	3.8	4.4	3.5 ± 0.3
4.40	1.31	17.5	27.7	4.0	4.0	2.7 ± 0.3
1.00	1.01	4.1	10.5	4.1	5.0	4.2 ± 0.4
						3.5 ± 0.7[f]
		333 K				
4.94	1.65	16.1	30.1	3.3	5.8	7.2 ± 2.5
6.78	1.42	31.5	34.7	4.6	5.2	
5.3	1.29	24.8	30.0	4.7	6.3	4.1 ± 1.5
0.53	0.75	2.2	14.0	4.1	2.9	9.2 ± 4.0[g]
		343 K				
5.08	1.27	14	30	2.7	9.2	$2.0^{2.0}_{-1.0}$

[a] Conditions: pressure = 1 atm. Cl_2 = 0.3 Torr; H_2 = 16 Torr; $ClNO_3$ = 0.003 Torr. [b] Maximum steady-state concentration during photolysis period, $[X]_{ss}$. [c] Initial pseudo-first-order rate constant d ln [X]/dt as "lamp off". [d] k_4 from k^1 values and $[X]_{ss}$. [e] k_4 from computer simulations using branching ratio $k_{4a} = k_{4b} = 0.5k_4$; 95% confidence limits derived statistically. [f] Average value. [g] Average value not given because fits not regarded as mechanistically reliable.

parameters which give the best fit to input experimental data.

The complete chemical scheme employed in the simulations is given in Table II. In addition to the reactions already discussed, the scheme included the reaction

$$H + Cl_2 \rightarrow HCl + Cl \qquad (17)$$

since this reaction affects the relative rates of HO_2 and NO_3 production via reactions 6 and 1. Reactions of Cl with NO_3 and with HO_2 were taken into account as well as the subsequent chemistry of ClO and OH produced in these reactions, including the reactions of these radicals with NO_3. Thermal decomposition of $ClONO_2$, N_2O_5 and HO_2NO_2 became important only at the higher temperatures employed. The photolysis of NO_2 and NO_3 was neglected because the removal of these species was dominated by their reaction with other radicals. The rate constants for the reactions in Table II were taken mostly from the most recent NASA evaluation;[18] other sources are referenced in Table II.

The experimental data input were the absorption–time profiles for HO_2 and NO_3, measured under specified conditions of temperature and composition. Absorptions at 20 equally spread time points were used for fitting. The radical absorption profiles were calculated within the program from the simulated concentration–time dependence using appropriate values for the absorption cross sections of HO_2 and NO_3. The values used were respectively 4.0×10^{-18} cm^2 molecule^{-1} at 220 nm[18] and 1.8×10^{-17} cm^2 molecule^{-1} at 662 nm. This value of σ_{NO_3} was determined in the present apparatus by using the same technique as we have reported previously[12] and agrees with the majority of the recent determinations. Use of a value of $\sigma_{NO_3} = 2.3 \times 10^{-17}$ cm^2 reported by Sander[19] gave values of k_4 from the computer simulations which were typically 6%–17% higher than those obtained with the above value.

The concentrations of Cl_2, $ClONO_2$, H_2, O_2, and N_2 were entered in the simulations as parameters with values equal to the mean concentration present in the reaction cell; for Cl_2 and $ClONO_2$ the average measured concentrations during modulated photolysis of the flowing mixture were used and for H_2, O_2, and N_2 the initial concentrations were used since the concentration changes were insignificant compared to the total. The other

TABLE II: Mechanism Used in Computer Simulations of Photolysis of Cl_2–$ClNO_3$–H_2–O_2 Mixtures

reaction	k/cm^3 molecule^{-1} s^{-1}, 298 K	(E/R)/K
$Cl_2 + h\nu \rightarrow 2Cl$	0.5×10^{-4} s^{-1} per lamp	
$Cl + H_2 \rightarrow HCl + H$	1.6×10^{-14}	2300
$H + O_2$ (+M) $\rightarrow HO_2$	1.1×10^{-12}	0
$H + Cl_2 \rightarrow HCl + Cl$	2.1×10^{-11}	0
$H + NO_3 \rightarrow OH + NO_2$	1.2×10^{-10}	0
$HO_2 + HO_2 \rightarrow H_2O_2 + O_2$	2.8×10^{-12}	−700
$Cl + ClONO_2 \rightarrow Cl_2 + NO_3$	1.2×10^{-11}	−160
$ClONO_2$ (+M) $\rightarrow ClO + NO_2$	4.4×10^{-3} s^{-1}	11 820
$ClO + NO_2$ (+M) $\rightarrow ClONO_2$	2.1×10^{-12}	0
$Cl + NO_3 \rightarrow ClO + NO_2$	5.5×10^{-11}	0[a]
$ClO + NO_3 \rightarrow Cl + O_2 + NO_2$	4.0×10^{-13}	420[a]
$OH + NO_3 \rightarrow HO_2 + NO_2$	2.6×10^{-11}	0[b]
$HO_2 + NO_3 \rightarrow HNO_3 + O_2$ / $\rightarrow OH + NO_2 + O_2$	see text	
$NO_2 + NO_3$ (+M) $\rightarrow N_2O_5$	1.2×10^{-12}	0
N_2O_5 (+M) $\rightarrow NO_2 + NO_3$	0.05 s^{-1}	11 153
$NO_2 + HO_2$ (+M) $\rightarrow HO_2NO_2$	1.3×10^{-12}	0
HO_2NO_2 (+M) $\rightarrow HO_2 + NO_2$	0.10 s^{-1}	10 870
$Cl + HO_2 \rightarrow HCl + O_2$	3.5×10^{-11}	−170
$\rightarrow ClO + OH$	9.0×10^{-12}	450
$ClO + HO_2 \rightarrow HOCl + O_2$	5.0×10^{-12}	−710
$OH + H_2 \rightarrow H_2O + H$	6.7×10^{-15}	2030
$OH + Cl_2 \rightarrow HOCl + Cl$	6.8×10^{-14}	911[c]
$OH + ClONO_2 \rightarrow HOCl + NO_3$	3.9×10^{-13}	333
$OH + H_2O_2 \rightarrow H_2O + HO_2$	1.7×10^{-12}	187
$OH + HOCl \rightarrow H_2O + ClO$	1.8×10^{-12}	150
$OH + HO_2NO_2 \rightarrow H_2O + NO_2 + O_2$	4.6×10^{-12}	380
$Cl + HOCl \rightarrow Cl_2 + OH$	1.9×10^{-12}	130
$Cl + HO_2NO_2 \rightarrow HCl + NO_2 + O_2$	5.0×10^{-11}	0[d]

[a] Reference 11. [b] Reference 16. [c] Reference 20. [d] Estimated.

(19) Sander, S. P. *J. Phys. Chem.* **1986**, *90*, 4135.
(20) Boodaghians, R. B.; Hall, I. W.; Wayne, R. P. *J. Chem. Soc., Faraday Trans. 2* **1987**, *83*, 529.
(21) Stimpfle, R.; Perry, R.; Howard, C. J. *J. Chem. Phys.* **1979**, *71*, 5183.

TABLE III: Values of the Rate Constant k_4 Obtained by Computer Fitting the NO_3 and HO_2 Absorption Profiles Using Two Alternative Channels for the $NO_3 + HO_2$ Reaction

temp/K	$[NO_3]_{ss}{}^a/10^{12}$ molecules cm^{-3}	$[HO_2]_{ss}{}^a/10^{12}$ molecules cm^{-3}	$k_{4a}/10^{-12}$ $cm^3\ s^{-1}$	$\sum r^{2b}$	$k_{4b}/10^{-12}$ $cm^3\ s^{-1}$	$\sum r^{2b}$
263	0.99	0.77	6.3 ± 0.9	38.1	4.0 ± 0.7	10.1
283	1.54	1.06	5.7 ± 0.8	26.3	5.4 ± 0.5	9.8
308	0.82	1.5	4.3 ± 0.4	7.3	3.2 ± 0.3	8.7
333	1.29	5.30	5.0 ± 1.8	27.4	4.2 ± 1.6	29.0

[a] Maximum steady-state concentrations during photolysis. [b] Sum of squares of residuals from all 40 experimental points.

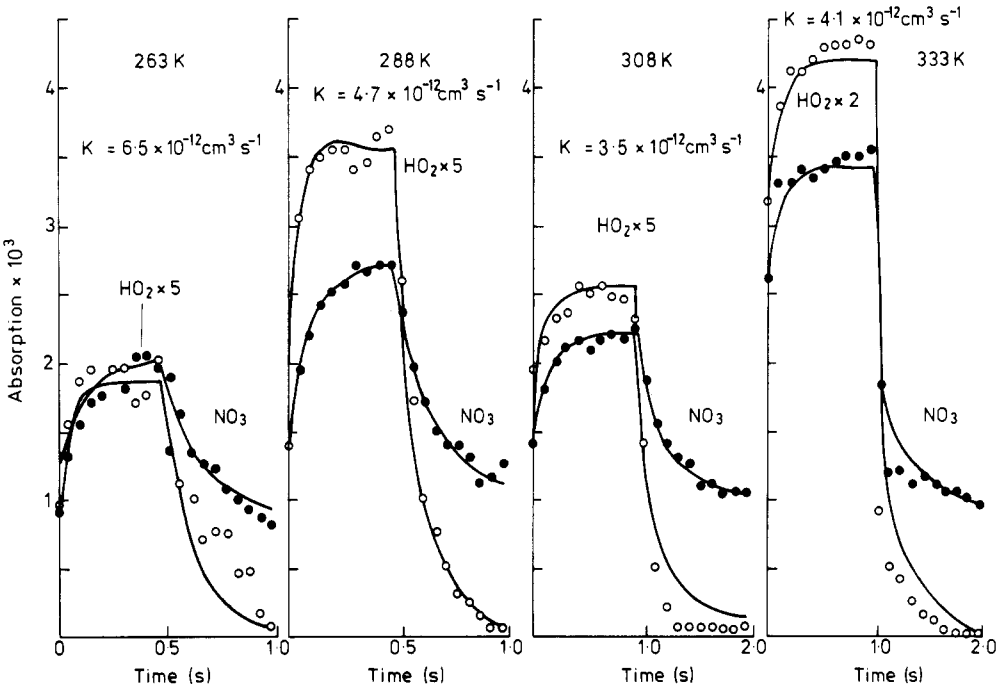

Figure 3. Computer simulations of NO_3 and HO_2 absorption–time profiles at four temperatures. Also shown are "best fit" values of the overall rate coefficient k_4 with assumed branching ratio $k_{4a}/k_{4b} = 1$.

species, NO_3, H, HO_2, OH, NO_2, Cl, ClO, H_2O_2, HO_2NO_2, HOCl, HNO_3, N_2O_5, and HCl, were all treated as variables and started at zero concentration. All rate constants except k_4 were specified.

The experimental NO_3 data included the residual absorption estimated from the chart recorder trace, but for HO_2 only the modulated absorption was fitted. Since the NO_3 residuals were small and could not be estimated accurately, this quantity was allowed to vary in the simulation. In order that the steady-state radical absorptions could be fitted accurately, the photolysis rate was allowed to vary, although it was found that the "best fit" value was in most cases close to the value entered. It was also necessary to allow the parameterized average chlorine nitrate concentration to vary to obtain the correct relative amounts of HO_2 and NO_3. In most cases this parameter did not change significantly during the fitting iteration.

The main variable of interest was the rate constant k_4. Simulations were first conducted with a single channel of either k_{4a} or k_{4b}, and the results of some of these fits are shown in Table III. When the OH-forming route was used, the k_4 values tended to be lower by about 10%–15%. At the two lowest temperatures the best fit using the OH-forming route gave a significantly lower sum of squares of residuals than that using the HNO_3-forming route, the improvement being mainly due to a better description of the observed NO_3 profile. When both channels were included and allowed to vary independently, the resultant individual values were highly anticorrelated and had large uncertainties. It is concluded that distinction between the two channels in reaction 4 cannot be made from the kinetic results obtained in this study. The overall value of k_4 was well determined in all cases, however.

During the course of this work we learned of another study of the $NO_3 + HO_2$ reaction performed by Mellouki and co-workers,[16] using the discharge flow technique at low pressure with EPR detection of NO_3 and HO_2 (after titration with NO to give OH). In their study the branching ratio for OH formation could be determined directly from time-resolved measurements of OH concentration. The following values of the rate constants at 298 K were obtained: $k_{4a} = (9.2 \pm 4.8) \times 10^{-13}$ cm^3 $molecule^{-1}$ s^{-1} and $k_{4b} = (3.6 \pm 0.9) \times 10^{-12}$ cm^3 $molecule^{-1}$ s^{-1}. The value for the total rates is midway between the 283 and 308 K values derived from the present study (see Table III) and therefore shows excellent agreement. The ratio $k_{4b}/k_4 = 0.80$ is somewhat higher than suggested by our measurements of OH at 283 K.

TABLE IV: Rate Constants for Separate Channels in the $NO_3 + HO_2$ Reaction by Computer Fitting of NO_3 and HO_2 Absorption[a]

temp/K	$k_4{}^b$	$k_4{}^c$	$k_{4a}{}^c$	$k_4{}^d$
263	6.5 ± 0.5[e]	4.9 ± 0.7	0.9 ± 0.7	5.0
283	4.7 ± 0.8	4.9 ± 0.9	1.1 ± 0.7	4.4
308	3.5 ± 0.7	3.7 ± 0.5	0.6 ± 0.4	4.2
333	6.8 ± 2.7	$6.4^{3.5}_{-3.1}$	$3.1^{3.5}_{-3.1}$	4.6
343	$2.0^{+2.0}_{-1.0}$			5.9

[a] In units of 10^{-12} cm^3 $molecule^{-1}$ s^{-1}. [b] Fitted using $k_{4a} = k_{4b}$. [c] Fitted k_{4a} using k_{4b} based on Mellouki et al.[16] value at 298 K and an assumed $E/R = -250$ K. [d] Average values from analysis by eq i and ii in Table I. [e] Uncertainty limits reflect range of values obtained from different experiments.

In order to obtain the optimum values for k_4 from the data obtained in the present study, simulations were performed with two different assumptions concerning the branching ratio in reaction 4. First, a branching ratio of 0.5 was assumed for each channel and the overall k_4 allowed to vary. Second, k_{4b} was fixed at a value based on the 298 K value obtained by Mellouki et al. and an assumed E/R of −250 K and k_{4a} allowed to vary.

The results of these simulations are given in Table IV, and some typical examples of the match between computed and experimental

TABLE V: Temperature Dependences of HO_2 + Radical Reactions

reaction	(E/R)/K
Reactions Involving H-Atom Transfer	
$HO_2 + OH \rightarrow H_2O + O_2$	-416 ± 200^a
$HO_2 + HO_2 \rightarrow H_2O_2 + O_2$	-590 ± 200^a
$HO_2 + ClO \rightarrow HOCl + O_2$	-710 ± 250^b
$HO_2 + NO_3 \rightarrow HNO_3 + O_2$	-170 ± 270
Reactions Involving O-Atom Transfer	
$HO_2 + O \rightarrow OH + O_2$	-200 ± 200^a
$HO_2 + NO \rightarrow OH + NO_2$	-240 ± 80^a
$HO_2 + NO_3 \rightarrow OH + NO_2 + O_2$	-170 ± 270

[a] Reference 18. [b] Reference 21.

data are shown in Figure 3. An excellent fit to the data with good convergence was obtained for all of the individual experiments at the three lowest temperatures; when k_{4b} was fixed, the occurrence of the HNO_3-forming channel was clearly indicated by the data. At the higher temperatures the fits, as reflected in the residual sums of squares, were not so good. The values of k_4 at 333 and 343 K all had larger uncertainty limits, and the observed steady-state concentrations of HO_2 and NO_3 could only be reproduced in the model with unreasonably high photolysis rates and chlorine nitrate concentrations. It would appear that the mechanism used does not give a complete description of the chemistry in the present system at the higher temperatures, but we are unable to suggest a plausible explanation of the origin of the problem. However, the average values of k_4 obtained from the decay of HO_2 and NO_3 from the steady states (i.e., from eq i and ii) give reasonably consistent values of k_4 at all temperatures.

The better defined low-temperature data in Table IV give an indication of a negative temperature dependence of k_4, but in view of the uncertainty on the higher temperature data, a firm conclusion regarding the temperature dependence cannot be drawn. Least-squares analysis of all the fitted values of k_4 and the average values from analysis of the NO_3 decay curves given in Table IV gives an Arrhenius expression for k_4:

$$k_4 = (2.3^{+2.8}_{-1.8}) \times 10^{-12} \exp(+(170 \pm 270)/T)\ \mathrm{cm^3\ molecule^{-1}\ s^{-1}}$$

(Error = 2 standard deviations.) The uncertainty on the Arrhenius parameters allows for the possibility that k_4 is temperature independent. Nevertheless, our data are consistent with a small negative temperature dependence for the overall rate constant k_4.

A negative temperature dependence for the $NO_3 + HO_2$ reaction is in line with the general pattern for exothermic bimolecular reactions of HO_2 with small radicals (see Table V). The reactions of HO_2 with OH, HO_2, and ClO all involve H-atom transfer which is believed to occur via internal rearrangement of a short-lived addition complex. The reaction between NO_3 and HO_2 to give HNO_3

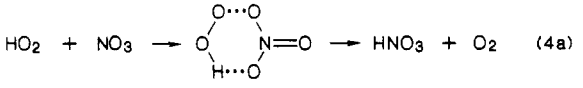

would be expected to be of this type and may by analogy have a substantial negative temperature dependence. The O-atom transfer reactions of HO_2 (e.g., with $O(^3P)$ and NO) exhibit less temperature dependence ($E/R \approx -200$ K). If the analogous reaction with NO_3

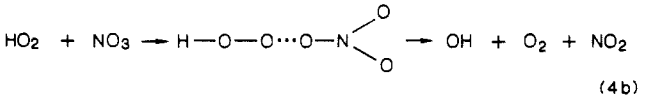

possessed a similar temperature dependence, then the small negative temperature dependence indicated in the present study for the overall reaction would be consistent with a major contribution of the OH-forming channel to the overall rate constant.

It is also of interest to compare the kinetics of reaction 4 with the reaction of NO_3 with ClO, which has recently been studied in our laboratory:[11]

$$NO_3 + ClO \rightarrow NO_2 + ClOO \quad (18a)$$

$$\rightarrow NO_2 + OClO \quad (18b)$$

The overall reaction is approximately a factor of 10 slower than the $HO_2 + NO_3$ reaction at room temperature and has a small positive temperature dependence: $k = 1.6 \times 10^{-12} \exp(-420/T)$. The major channel is the more exothermic route forming ClOO. Exothermic channels involving Cl-atom transfer, analogous to HNO_3 formation via a cyclic complex in the $NO_3 + HO_2$ reaction, are not possible in the reaction with ClO. Therefore, this reaction probably occurs by a similar mechanism to reaction 4b:

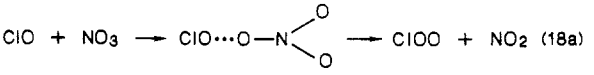

and the A factors should be of similar magnitude. The A factor for reaction 18 is indeed close to that for reaction 4. Better definition of the temperature dependences of these reactions is required to confirm these suggested mechanisms for the reactions of NO_3 with other radicals.

The nitrate radical is formed throughout the atmosphere by the reaction of NO_2 with O_3:

$$NO_2 + O_3 \rightarrow NO_3 + O_2 \quad (19)$$

NO_3 is rapidly photolyzed by visible radiation and consequently, in the daytime, reactions of NO_3 with HO_2, ClO, and other photochemically generated radicals (except NO) are of minor importance. For example, typical daytime concentrations of HO_2 in the troposphere and in the midstratosphere are $\sim 10^8$ molecules cm^{-3}, giving an effective loss rate of NO_3 of $0.5 \times 10^{-3}\ s^{-1}$ via reaction 4, compared with $0.2\ s^{-1}$ for photodissociation. At night, free-radical concentrations fall rapidly and NO_3 loss by reaction with radicals will be much slower. Nevertheless, since NO_3 photolysis does not occur in the dark, the radical + NO_3 reactions may become significant.

The effect of reaction 4 on stratospheric chemistry will depend on the product channels; HNO_3 formation will lead to overall loss of O_3, HO_x, and NO_x, whereas formation of OH and NO_2 leads to loss of O_3 only, through the catalytic cycle

$$NO_2 + O_3 \rightarrow NO_3 + O_2 \quad (19)$$

$$HO_2 + NO_3 \rightarrow OH + NO_2 + O_2 \quad (4b)$$

$$OH + O_3 \rightarrow HO_2 + O_2 \quad (20)$$

net: $$2O_3 \rightarrow 3O_2$$

Although these reactions contribute only a minor amount to the total O_x, NO_x, and HO_x budgets in stratosphere, there is a need to improve the accuracy of the rate constant k_4 and determine the temperature dependence of the branching ratio.

Acknowledgment. This work was carried out on a program of atmospheric chemistry research funded by the U.K. Department of the Environment (DOE). I.W.H. thanks the DOE for Post Graduate Support at the Physical Chemistry Laboratory, Oxford.

Registry No. NO_3, 12033-49-7; HO_2, 3170-83-0.